Published in final edited form as:

Breast Cancer Res Treat. 2021 August ; 188(3): 615–630. doi:10.1007/s10549-021-06239-y.

Early Assessment Window for Predicting Breast Cancer Neoadjuvant Therapy using Biomarkers, Ultrasound, and Diffuse Optical Tomography

Quing Zhu[1,2], **Foluso O. Ademuyiwa**[3], **Catherine Young**[4], **Catherine Appleton**[5], **Matthew F. Covington**[6], **Cynthia Ma**[3], **Souzan Sanati**[7], **Ian S. Hagemann**[8], **Atahar Mostafa**[1], **K. M. Shihab Uddin**[1], **Isabella Grigsby**[3], **Ashley E. Frith**[3], **Leonel F. Hernandez-Aya**[3], **Steven S. Poplack**[2,9]

[1]Biomedical Engineering and Radiology, Washington University in St Louis, One Brookings Drive, Mail Box 1097, Whitaker Hall 200F, St. Louis, MO 63130, USA

[2]Washington University School of Medicine in St Louis, St. Louis, USA

[3]Medical Oncology, Washington University School of Medicine in St Louis, St. Louis, USA

[4]Washington Baylor Scott & White Health, Medical Center, Texas, Dallas, USA

[5]Diagnostic Imaging Associates, Ltd. St. Luke's Hospital, Chesterfield, USA

[6]Department of Radiology and Imaging Sciences, University of Utah, Salt Lake City, USA

[7]Pathology, Department of Pathology, Cedars-Sinai Medical Center, Los Angeles, USA

[8]Washington University School of Medicine in St Louis, St. Louis, USA

Quing Zhu, zhu.q@wustl.edu.

Author contributions QZ: designed and conducted all aspects of the ultrasound-guided optical tomography data acquisition, image reconstruction and data analysis and contributed to the manuscript preparation and literature review. SPP: designed and conducted patient imaging studies, data analysis, and contributed to the manuscript preparation and literature review. FOA and CM: coordinated and recruited patients to the study, and contributed to the manuscript review and literature review. CY, CA, MFC: contributed to the imaging studies, imaging interpretations, and manuscript review. SS and ISH: contributed to the pathological data evaluations, interpretations, manuscript review. AM and K.M.S.U: contributed to the development of optical tomography system hardware and software as well as imaging algorithm. IG: coordinated, consented all study patients, and data analysis. AEF and LFH: contributed to patient recruitments. All authors read and approved the final manuscript.

Conflict of interest QZ is the inventor of the patents related to ultrasound-guided near-infrared tomography technologies and patents owned by the University of Connecticut and/or Washington University in St Louis. She has no conflicts of interest. All authors declare that they have no conflicts of interests.

Code availability The code is available from the corresponding author on reasonable request.

Ethical approval All procedures performed in studies involving human participants were in accordance with the ethical standards of the institutional and/or national research committee and with the 1964 Helsinki declaration and its later amendments or comparable ethical standards.

Informed consent Informed consent was obtained from all individual participants included in the study.

Research involving human and animal rights This article does not contain any studies with animals performed by any of the authors.

Consent for publication All authors have read the manuscript and agreed with the submission.

Publisher's Note Springer Nature remains neutral with regard to jurisdictional claims in published maps and institutional affiliations.

Clinical Trial Registration number:NCT02891681. https://clinicaltrials.gov/ct2/show/NCT02891681,Registration time: September 7, 2016

Supplementary Information The online version contains supplementary material available at https://doi.org/10.1007/s10549-021-06239-y.

[9]Present Address: Radiology, Stanford University, Stanford, USA

Abstract

Purpose—The purpose of the study was to assess the utility of tumor biomarkers, ultrasound (US) and US-guided diffuse optical tomography (DOT) in early prediction of breast cancer response to neoadjuvant therapy (NAT).

Methods—This prospective HIPAA compliant study was approved by the institutional review board. Forty one patients were imaged with US and US-guided DOT prior to NAT, at completion of the first three treatment cycles, and prior to definitive surgery from February 2017 to January 2020. Miller-Payne grading was used to assess pathologic response. Receiver operating characteristic curves (ROCs) were derived from logistic regression using independent variables, including: tumor biomarkers, US maximum diameter, percentage reduction of the diameter (%US), pretreatment maximum total hemoglobin concentration (HbT) and percentage reduction in HbT (%HbT) at different treatment time points. Resulting ROCs were compared using area under the curve (AUC). Statistical significance was tested using two-sided two-sample student *t*-test with $P < 0.05$ considered statistically significant. Logistic regression was used for ROC analysis.

Results—Thirty-eight patients (mean age = 47, range 24–71 years) successfully completed the study, including 15 HER2 + of which 11 were ER + ; 12 ER + or PR + /HER2−, and 11 triple negative. The combination of HER2 and ER biomarkers, %HbT at the end of cycle 1 (EOC1) and %US (EOC1) provided the best early prediction, AUC = 0.941 (95% CI 0.869–1.0). Similarly an AUC of 0.910 (95% CI 0.810–1.0) with %US (EOC1) and %HbT (EOC1) can be achieved independent of HER2 and ER status. The most accurate prediction, AUC = 0.974 (95% CI 0.933–1.0), was achieved with %US at EOC1 and %HbT (EOC3) independent of biomarker status.

Conclusion—The combined use of tumor HER2 and ER status, US, and US-guided DOT may provide accurate prediction of NAT response as early as the completion of the first treatment cycle.

Keywords

Predicting neoadjuvant therapy; Personalized medicine; Near Infrared imaging; Ultrasound

Introduction

Preoperative neoadjuvant therapy (NAT) for patients with locally advanced breast cancer downstages the tumor to facilitate breast conserving surgery, and allows in vivo assessment of therapeutic efficacy for tailored treatment approaches. Pathological response to NAT predicts clinical outcome. An absence of residual invasive breast cancer cells, in the primary tumor bed and lymph nodes following NAT is strongly correlated with improved disease-free survival and overall survival [1]. However, breast cancer is a heterogeneous disease; approximately 20–25% of breast cancers have amplification of the human epidermal growth factor receptor 2 (HER-2/neu), while 10–20% of breast cancers lack expression of estrogen receptor and progesterone receptor and HER2 gene amplification, known as triple-negative breast cancer (TNBC). Dual HER2 blockade in the neoadjuvant setting has been shown to increase the pathological complete response (pCR) rate in HER2 positive disease [2–4]. Despite this, there is a significant percentage of HER2 + patients who do not achieve

a pCR or near pCR [5]. Those patients who have residual invasive breast cancer after HER2-targeted therapies have a worse prognosis [6]. Moreover, to date, no FDA-approved targeted therapies are available for early-stage TNBC patients and refining TNBC breast cancers into molecular subtypes still is a significant challenge in predicting NAT [7]. Thus, there is an unmet need for individual assessment before and during early NAC to guide treatment options by switching patients to other therapies to achieve optimal outcomes with reduced toxicity.

Many ongoing investigations are exploring imaging techniques to monitor response. The use of imaging is appealing because it is non-invasive and may provide a window of opportunity wherein ineffective treatment regimens could be altered. Conventional imaging methods include mammography, ultrasound (US), MRI and PET-CT. Mammography has low sensitivity in the evaluation of NAT response [8]. US is moderately accurate [9–12] and has the additional benefits of easy access and low cost. MRI and PET-CT have both demonstrated good accuracy in predicting pCR [13–15], however, both are cost prohibitive given the need for serial imaging evaluation.

Optical tomography and spectroscopy using near infrared (NIR) diffused light has been explored as a novel tool to predict and monitor tumor vasculature response to NAT [16–26]. The NIR technique utilizes intrinsic hemoglobin contrast, which is related to tumor angiogenesis. Recently studies have shown that pre-treatment total hemoglobin concentration (HbT) and changes in HbT measured at the early treatment cycles can predict treatment outcome [16–26]. Furthermore, the Diffuse Optical Tomography (DOT) can be easily integrated with ultrasound systems for dual-modality imaging assessment of breast cancer response to NAT. This manuscript reports a three-year prospective study of a considerable patient population evaluated with US and US-guided DOT before, during, and after treatment completion in an attempt to identify the best and earliest predictors of pCR for HER2+, ER+/HER2− and triple negative breast cancer subtypes.

Materials and methods

Patient

This prospective study was approved by the local institutional review board and was HIPAA compliant. Sixty female patients with newly diagnosed breast cancer presenting to medical oncology at Washington University School of Medicine from February 2017 to August 2019 for preoperative systemic therapy signed informed consent. Exclusion criteria were given in Fig. 1 and fifteen patients were subsequently deemed ineligible and four patients withdrew. Of the remaining 41 patients, two developed metastases and did not complete the study and one had a contralateral abnormality preventing reference imaging. Data from these three patients were not included in the analysis. Thus 38 female patients (mean age = 47, range 24–71 years) constituted the study group and underwent US and US-guided DOT imaging of the index breast cancer prior to the initiation of NAT, at the end of the first three treatment cycles and before definitive surgery. Patients were treated with NAT regimens according to current clinical practice or based on therapeutic trial protocols.

Baseline imaging was performed an average of 28 days after diagnostic core needle biopsy (median = 26, range 7–56 days) and before the first treatment (median = 1 day, range 0–15 days). During treatment, imaging occurred before patient scheduled treatment (median = 0, range 0–5 days). The average interval between post-treatment imaging and definitive surgery was 25 days (median 20, range 1–163 days).

US and US-guided DOT imaging

Ultrasound and US-guided DOT examinations were completed in a breast imaging clinic with 4 commercial US units and associated US probes of SL15–4 (Aixplorer™, Super-Sonic Imagine Inc., Aix-en-Provence, FR) and a 4th generation DOT system. Standard US was performed by one of four dedicated breast imaging radiologists with an average of 12 years of breast US experience (range 2–24 years) at study initiation. The index tumor was imaged in orthogonal planes and the maximum diameter was recorded. Prior US examinations were referenced during the exam to ensure consistency of measurements. The percentage ratio %US, largest dimension of each post-treatment time point over the largest dimension pretreatment, was used to evaluate the fraction reduction from NAT. After completion of the breast US examination, the commercial US probe was inserted into the DOT probe. The breast radiologist then directed the engineer to the index tumor site and assisted in US-guided DOT acquisition as needed.

Details of the 4th generation DOT system used for this trial have been previously reported [27]. Briefly, the US-guided DOT hand-held probe consists of the commercial US transducer located centrally, with source and detector optical fibers distributed around the periphery (see Fig. 2). The entire data acquisition from 9 source positions and 14 detectors was less than 4 s. For each patient, US images and optical measurements were acquired simultaneously of both the index tumor site and subsequently a normal region within the corresponding quadrant of the contralateral breast. Multiple datasets were acquired of the index tumor and contralateral reference site. The perturbation caused by tumor between the measurements of the tumor site and the reference site was used for image reconstruction. The measurements from the normal contralateral breast were used for calculating the background optical absorption and reduced scattering coefficients which were used for computing weight matrix for image reconstruction.

The US-guided DOT reconstruction algorithm has been reported [22, 28]. In brief, the DOT reconstruction uses ultrasound lesion identification to segment the imaging volume into a region of interest (ROI) and background to improve the inversion. The ROI is two to three times larger in spatial dimensions than the tumor size (as measured by co-registered US) due to the low spatial resolution of diffused light. A tighter ROI in the depth dimension is set by using co-registered US. The pretreatment ROI is used for data processing of all time points, thereby minimizing the effect of treatment related changes in tumor size on the optical image reconstruction.

The optical absorption distribution at each wavelength was reconstructed, and the total hemoglobin concentration (HbT), oxygenated-hemoglobin (oxyHb) and deoxygenated-hemoglobin concentration (deoxyHb) maps were computed. An average maximum value of HbT, oxyHb, and deoxyHb was obtained from 5 to 10 optical images reconstructed from

each of the separate repetition of measurements acquired from the index tumor. Data with patient motion were recognized by using two co-registered US images before and after each optical data set and were excluded from averaging. To assess each patient's response, the HbT obtained before treatment was taken as the baseline and the percentage (%HbT) normalized to the baseline was used to quantitatively evaluate the remaining tumor vascular fraction during NAT.

Pathology assessment

Pathology data were extracted from pathology reports and from re-examination of formalin-fixed, paraffin-embedded slides to complete missing data. One breast pathologist (SS, 10 years experience) evaluated cases from patients recruited between February 2017 to May 2019 and the second breast pathologist (ISH, 7 years experience) evaluated the rest. Response to NAT in each surgical resection specimen was graded using Miller-Payne (MP) criteria [29], with comparison to initial core biopsy when necessary. There are five MP grades based on reduction in tumor cellularity: Grade 1—no change or minor alteration in individual malignant cells but no reduction in overall cellularity. Grade 2—minor (up to 30%) loss of tumor cells but overall cellularity remains high. Grade 3—estimated 30% to 90% reduction in tumor cells. Grade 4—marked (> 90%) disappearance of tumor cells or near pCR. Grade 5—no malignant cells are identifiable in sections from the tumor bed (pCR). The MD Anderson residual cancer burden (RCB) was calculated based on the primary tumor bed, overall cancer cellularity, in situ disease, number of positive lymph nodes and diameter of the largest lymph node metastasis [30]. Since US and US-guided DOT were performed on the index tumor, the MP grading system was used to evaluate pathological response and RCB was used as a reference for MP grade.

Invasive carcinoma within the pretreatment core biopsies was graded using the Nottingham histologic score (NS). Testing for estrogen receptor (ER), progesterone receptor (PR), and HER2/neu (c-erbB-2) expression was performed by immunohistochemistry by an FDA-approved method on formalin-fixed, paraffin-embedded pretreatment core biopsy tissue. The ER and PR were scored by Allred scoring system [31], where the total score ranges from 0 to 8 (scores ≥ 3 are positive). HER2 was scored in accordance with 2018 ASCO/CAP guidelines. Cases with equivocal HER2 immunostaining were reflexed to fluorescence in situ hybridization (FISH).

Statistical analysis

Generalized Logistic Regression (Eq. 1) was used to relate treatment outcomes to individual predictor variables for ROC analysis [32]. Briefly, logistic regression describes the relationship of several predictor variables $X_1, X_2 \ldots X_k$ to a dichotomous response variable Y (1: responder, 0: non-responder). The model can be written in the form of the conditional probability of the occurrence of one of the two possible outcomes of Y, as follows:

$$pr(Y = 1 \mid X_1, X_2, \ldots X_k) = \frac{1}{1 + \exp(-\left(\beta 0 + \sum_{n=1}^{k} \beta n X n\right)} \quad (1)$$

Given the data on $Y, X_1, \ldots X_k$, the unknown parameters β_n, n = 0, 1, …k can be estimated using the maximum likelihood method and an ROC is obtained from the regression output.

Spearman is a rank based Pearson and is used for continuous or ordinal variables [32]. Because binary predictor variables can be viewed as special ordinal variables, Spearman's rho correlation coefficient is used for assessing predictors in our study. Each predictor was first correlated with the MP grade using Spearman's rho to assess its predictive value. The t-test was used to evaluate the statistical significance and *P* values less than 0.05 were considered significant. For each pair of significant predictors, a correlation between the two predictors was evaluated using Spearman's rho. The correlated predictors with Spearman's rho greater than 0.6 were not used together for ROC analysis. Minitab 19 software (Minitab, State College, PA) was used for ROC and statistical calculations. The 95% confidence interval (CI) of each ROC was computed in R using the pROC package. To evaluate the significance of different ROCs with different sets of predictors, we used a function deltaAUC in R, which was specially designed to compare AUCs with overlapping predictors [33].

When comparing %HbT and %US at different treatment cycles, the Bonferroni-Holm correction was applied to obtain the corrected *P* value as $Pc(\mathrm{i}) = (n - \mathrm{i} + 1) \times P(i) < \alpha$, where α is 0.05, *n* is 3 which corresponds to the first three treatment cycles. i starts from 1 (corresponding to the smallest *P* value) to 3 (corresponding to the largest *P* value).

In Online Appendix, we developed treatment prediction models using a supervised machine learning method based on logistic regression (Eq. 1). Data of 38 patients reported in this study and 22 patients acquired in an earlier study with similar DOT system parameters, patient and treatment characteristics [19] were used to train and then test the prediction models for generalizing the models [34].

Results

Table 1 summarizes patient and tumor characteristics, NAT regimens and MP grading. The histologic type of 35 patients was invasive ductal carcinoma of no special type; one patient had invasive mucinous carcinoma, one patient had invasive lobular carcinoma and one patient had invasive mammary carcinoma with mixed ductal and lobular features. One of the 38 patients had multi-focal disease consisting of three adjacent distinct tumor masses with identical histology. For this patient, the largest of the three masses was used for data analysis. Fifteen patients were HER2 + , 11 were triple-negative (TNBC), and 12 were ER + /HER2 − (*n* = 10) or PR + /HER2 − (*n* = 2). Eight patients had stage 3 disease, 27–stage 2, and 3–stage 1. For the three patients with stage 1 disease, two had HER2 + tumors, and one had high grade TNBC. Based upon MP grade, 5 patients had no response (pNR) (MP1), 11 patients had a partial response (pPR), including 3 with a minor response (MP2) and 8 with an intermediate response (MP3), while 3 had a near pCR (MP4) and 19 had a pCR (MP5). Tumor characteristics, US and optical parameters were correlated to MP grades using the Spearman's rho correlation (Table 2). We have dichotomized MP1–3 to non- or incomplete response, referred as non-responders, MP4–5 to complete response, referred

as complete responders. Spearman's rho correlation coefficients of all pairs of treatment prediction variables were given in Table 3.

HER2 + and ER + /HER2– status was significantly associated with MP-grade ($P = 0.039$, $P = 0.036$), while Nottingham grade and TNBC were not predictive ($P = 0.115$, $P = 0.138$). Pretreatment maximum tumor size measured by US was predictive ($P = 0.011$). MP1–3 had a baseline maximum of 34.4 mm ± 12.8 mm, vs. 26.9 mm ± 10.9 mm for MP4–5, but the difference between the two responder groups was not statistically significant ($P = 0.066$). Reduction in tumor size %US at the end of each of the first three cycles was predictive of MP-grade ($P = 0.005$, $P = 0.045$, $P = 0.013$), especially at EOC1. Post-treatment %US was not predictive (P = 0.111), however, post-treatment tumor size was ($P = 0.012$). Pretreatment HbT correlated with MP–grade ($P = 0.028$), while oxyHb and deoxyHb were not ($P = 0.091$, $P = 0.132$). Reduction in HbT (%HbT) showed the strongest correlation with MP–grade at the end of each of the first three cycles ($P = 0.001$, $P < 0.001$, $P < 0.001$). Post-treatment %HbT also showed a strong correlation with MP–grade ($P = 0.007$).

Figure 3 demonstrates the HbT, reduction in HbT, %HbT, and reduction in tumor size, %US, over the first three treatment cycles. Bonferroni-Holm correction was applied to adjust for multiple comparisons of %HbT and %US over treatment cycles. There was a significant difference in pretreatment mean maximum HbT between MP4–5 (85.9 μM ± 20.0) vs. MP1–3 (71.3 μM ± 19.1) ($P = 0.029$) (Fig. 3a). However, there was no difference at EOC1 or EOC2 ($P = 0.870$, $P = 0.194$) because the mean HbT level decreased at a faster rate in complete responders. At EOC3 complete responders had a significantly lower HbT ($P = 0.001$). The faster rate of reduction is best visualized in Fig. 3b. MP4–5 tumors decreased rapidly to 78% (of baseline)± 18.9, 64.2%± 18.5, 48.2 ± 13.8 at EOC1, EOC2 and EOC3, respectively, whereas MP1–3 tumors changed minimally to 97.3%± 22.6 (EOC1), 88.7% ± 22.9 (EOC2), and 89.0%± 26.4(EOC3). The differences between the two groups were increasingly significant as treatment progressed through the first three cycles; Pc = 0.012 (EOC1), Pc = 0.008 (EOC2) and Pc < 0.001 (EOC3), respectively.

The %US measurements showed a similar trend. The reduction in diameter was significant with reduction rate of 74.8%± 17.8, 61.8%± 28.3, 52.4%± 29.4 in MP4–5 tumors and 96.5%± 17.8, 82.4%± 23.7 and 74.7%± 23.5 in MP1–3 tumors, respectively (Fig. 3c). The differences between the two groups were significant with Pc = 0.003 (EOC1), Pc = 0.028 (EOC2), Pc = 0.040 (EOC3), respectively.

Examples of a treatment responder and a non-responder are shown in Figs. 4 and 5.

We performed ROC analyses using logistic regression (Eq. 1) to identify the best early predictors of response (MP4–5) at different treatment time points, EOC1–3. AUCs are tabulated (Table 4) with and without predictive biomarker status of ER and HER2, and subsets ROCs shown graphically in Fig. 6 with generalized logistic regression parameters, β_n, given in Table 5. As noted above HER2 and ER status were shown to predict treatment response without other imaging parameters (AUC = 0.773, 95% CI 0.629–0.917). When added to ER and HER2 status, %US at EOC1 noticeably improves the AUC (AUC = 0.883, 95% CI 0.768–0.997). Similarly, the addition of HbT and %HbT to biomarker

status substantially increases the AUC (AUC = 0.903, 95% CI 0.808–0.998). While each parameter is independently helpful, the combination of %US and %HbT is most effective in enhancing the prediction. The combination of predictive biomarkers, %US and %HbT at EOC1 provides the best prediction of response at the earliest time point, AUC = 0.941 (95% CI 0.869–1.0), which is significant when compared with biomarkers and %US at EOC1 ($P < 0.001$). The greatest AUC of any time during early treatment (AUC = 0.974, 95% CI 0.932–1.0) is achieved through the combination of predictive biomarkers, %US (EOC1) and %HbT (EOC3), which is also significant when compared with biomarkers and %US at EOC1 ($P < 0.001$). Even in the absence of ER and HER2 status, the identical maximum AUC is achieved (AUC = 0.974, 95% CI 0.933–1.0) using %US (EOC1) and %HbT (EOC3), with only slight diminution at the earliest time point, i.e. %US (EOC1) and %HbT (EOC1), AUC = 0.910 (95% CI 0.810–1.0). The AUC improvements of adding %HbT (EOC1) and %HbT (EOC3) to %US (EOC1) is statistically significant ($P < 0.001$). Note that MP–grade and RCB are highly correlated, Spearman's rho = 0.941 ($P < 0.001$). To develop a generalizable prediction model we have combined data from the 38 patients in this study with earlier data of a smaller patient population of 22 patients. Similar results were obtained (see Online Appendix).

Discussion

In current clinical practice, clinical breast examination, mammography, US, MRI, and PET-CT have been used to evaluate response in patients receiving NAT. Because of low cost and accessibility, US has been evaluated in several studies [9–12]. In a related study, Marinovich et al. evaluated 832 patients who underwent US at EOC2 and demonstrated an average increase in AUCs of 2% and 3% to 0.79 and 0.80 respectively, with the addition of US to patient characteristics including biomarkers [9]. In this study, we found that the fractional change of US maximum diameter (%US), measured at EOC1 (AUC = 0.83), was more predictive than EOC2 (AUC = 0.68). We further showed a substantial 11% increase, AUC = 0.77 to 0.88 at EOC1, in patients with known ER + or HER2 + disease. Our data show that early US measurements at EOC1 can substantially avoid measurement uncertainty as seen by smaller standard deviations of %US at EOC1 as compared to those at EOC2 and EOC3 for both responder and non-responder groups. In a recent paper, Dobruch-Sobczak et al. reported a series study of assessing US echogenicity, size, and other parameters of 19 tumors under NCT before treatment and after 7 days of each treatment course for up to 4 cycles [35]. They found that tumor echogenicity gradually increased from initially hypoechoic (all tumors) to mixed (hypo/isoechoic) and isoechoic tumors at a rate of 16% (3/19), 63% (12/19), 68% (13/19) and 72% (13/18) after each course of NCT. This texture change was caused by NCT-induced apoptosis of tumor cells, fibrosis, collagenization, and microcalcification. Tumor size was statistically significant between responders and non-responders after the first course ($P = 0.018$) but not at the second ($P = 0.102$) and the third course ($P = 0.149$). In another study, Matsuda et al. reported similar echogenicity changes during NCT but data were available only at the end of treatment cycle 4 [36]. We have observed a similar tread in echogenicity change as reported in [35] which increased uncertainty in US size measurements. Thus an optimal prediction window of NCT by %US could be as early as completion of one treatment cycle.

Diffuse optical tomography exploits changes in tumor vascularity and metabolism and have demonstrated the potential for early prediction of breast cancer pathological response [18–26]. Studies have shown accurate predictions in the neoadjuvant setting by utilizing pretreatment hemoglobin levels and changes in hemoglobin early in the course of treatment [19, 21–26], or by monitoring changes of blood oxygen saturation sO2 at day 1 of dose dense treatment [18] or day 10 during early treatment [20]. In the recent ACRIN 6691 trial evaluating 36 patients, the authors derived a tissue optical index (TOI), a product of deoxygenated Hb and water concentration over lipid, and reported that the mid-treatment TOI can predict pCR with AUC 0.6 to 0.83 [16]. Gunther et al. developed a dynamic diffuse optical tomography system that could identify patients with a pCR two weeks into the treatment with AUC = 0.85 [17]. In an earlier investigation of 22 patients [19], Zhu et al. identified HER2 status and HbT as the best pretreatment predictors of pCR (AUC = 0.88). With known HER2 positivity, the best window to accurately predict response was at the completion of the first and second cycles of NAT (AUC = 0.96, AUC = 0.97). For ER + /HER2− or TNBC subtype, the best window was at the completion of the first cycle of NAT and the best predictors were HbT and %HbT (AUC = 0.95).

In this new cohort of 38 patients, “HER2, ER and pretreatment HbT” has shown good prediction, AUC = 0.80 and “HbT alone” has shown moderate prediction AUC = 0.71. However, fractional reduction of HbT (%HbT) is a much more powerful predictor of response, as is fractional reduction of maximum diameter measured with US (%US) in the first three cycles. For chemo-sensitive tumors, NCT-induced neovasculature damage causes a significant and progressive decrease in tumor hemoglobin, as measured by the DOT system, and NCT-induced tumor tissue damage causes a significant size reduction, as measured by US. In particular, combining tumor HER2 and ER status, %US and %HbT at EOC1 provided the best early indicator of treatment response, AUC = 0.941, and remained powerful even without biomarker data, AUC = 0.910. With the assessment window extended to EOC3, the combination of %US EOC 3 and %HbT EOC3 provided accurate prediction, with AUC values of 0.969 with biomarker data and 0.944 without it. Overall, the highest accuracy, AUC = 0.974, was achieved with the combination of %US EOC1 and %HbT at EOC3, irrespective of biomarker status. To our knowledge, these AUC values are among the highest reported results using NAT regimens in current clinical practice.

The US-guided DOT has low intrinsic cost and is easily adaptable to clinical US systems. Disadvantages include: US-guided DOT imaging is not real-time and reconstruction currently takes 20 to 30 min. US-guided DOT is not suitable for imaging tumors in the dark nipple-areolar complex, and requires a sonographically visible tumor and normal contralateral reference tissue. Our study has a number of limitations. The treatment regimens were based on current practice at a research institution and were not limited to a single regimen. The choice of systemic therapies for breast cancer patients are based on multiple factors, including tumor biology, stage, patient characteristics and wishes, clinical trial availability. The study population was not large ($n = 38$) and to develop supervised machine learning prediction models detailed in Online Appendix, we included data from 22 patients from an earlier study with similar study criteria and patient characteristics [19]. Similar results were obtained. Only one patient was treated with an antiestrogen regimen, i.e.

anastazole, in our study cohort. Due to the limited sample size, we have grouped this patient with the rest of the patients and used pCR as surrogate endpoint.

In our previous work, we dichotomized our comparison groups as pCR and near pCR (MP4–5) versus non-responders (MP1–3) [19, 21, 22]. In this report, we have used the same comparison groups with the rationale given as follows: In the original study by Ogston [29] the MP 5 and 4 groups tended to track together with regard to 5 year disease free survive (DFS) after NCT and surgery (85% and 72%) versus 66%, 60% and 55% (for MP1–3). Later Zhao et al. [37], evaluating the MP system using a different dataset found very similar 5 year distant DFS and local recurrence-free survival rates for MP4–5 versus MP1–3. In a recent study, Sejben et al. [38] using the RCB system and another separate dataset also found the similar 5-year DFS for pCR and near-pCR (RCB-1) (85.2% and 84.4%) versus 58.2 and 33.0 for RCB-2 and RCB-3 and 5-year overall survival for pCR and near-pCR (94.4 and 87.7) versus 61.8 and 69.0 for RCB-2 and RCB-3 (RCB-2, partial response and RCB-3, chemoresistant).

Our study has substantial implications for the combined use of tumor subtypes, US and near-infrared-measured tumor hemoglobin content in accurately predicting pCR as soon as one treatment cycle is completed. A recently phase 3, open-label trial involving patients with HER2-positive early breast cancer who were found to have residual invasive disease has shown that adjuvant trastuzumab emtansine for 14 cycles reduced the risk of recurrence of invasive breast cancer or death by 50% as compared with trastuzumab alone [6]. Another trial of 910 HER2-negtive residual invasive breast cancer patients after neoadjuvant chemotherapy showed that adjuvant capecitabine was safe and effective in prolonging disease-free survival and overall survival [39]. If the residual disease could be accurately estimated earlier in the NCT, patients with an unsatisfactory response could be switched to investigational therapies or even definitive surgery as soon as cycle 1 is completed, allowing for personalized treatment. This ability will gain value as our armamentarium of interventions increases and responses can more effectively tailor the therapeutic agents selected.

Conclusion

In conclusion, our results suggest that the combination of HER2 and ER status, %HbT at the end of cycle 1 (EOC1) and %US (EOC1) accurately predict NAT (AUC = 0.941), and %HbT (EOC1) and %US (EOC1) predict NAT (AUC = 0.910) regardless of HER2 and ER status. A greater prediction accuracy can be achieved with AUC of 0.974 regardless of biomarkers when the treatment window is extended to EOC3. The synergistic use of US and US-guided DOT may provide a safe and low-cost strategy to accurately predict NAT outcomes early in the course of therapy.

Supplementary Material

Refer to Web version on PubMed Central for supplementary material.

Acknowledgements

The authors appreciate the help of Clinical Trial Office of the Oncology Department of Washington University School of Medicine for patient consenting and scheduling. Drs. Catherine Young, Catherine Appleton, Matthew F. Covington, were faculty members of Radiology Department of Washington University in St Louis from the beginning of the study to July 2019. Dr. Steven Poplack was a faculty member of Radiology Department of Washington University in St Louis from the beginning of the study to June 2020.

Funding

This study was funded by National Institutes of Health (R01EB002136, R01 CA228047). SPP acknowledges funding support from the Foundation for Barnes Jewish Hospital Ronald and Hanna Evens Endowed Chair in Women's Health.

Data availability

The patients' clinicopathologic characteristics are given in Table 1. The datasets generated during and/or analyzed during the current study are available from the corresponding author on reasonable request.

Abbreviations

NIR	Near infrared
pCR	Pathological complete response
ROI	Region of interest
ER	Estrogen receptor
PR	Progesterone receptor
HER2	Human epidermal growth factor receptor 2
TNBC	Triple-negative breast cancer
MP	Miller-Payne grade
RCB	Residual cancer burden
NAT	Neoadjuvant therapy
HbT	Total hemoglobin
ROC	Receiver operating characteristic curve
AUC	Area under receiving operating characteristic curve

References

1. Cortazar P, Zhang L, Untch M, Mehta K, Costantino JP, Wolmark N, Bonnefoi H, Cameron D, Gianni L, Valagussa P, Swain SM, Prowell T, Loibl S, Wickerham DL, Bogaerts J, Baselga J, Perou C, Blumenthal G, Blohmer J, Mamounas EP, Bergh J, Semiglazov V, Justice R, Eidtmann H, Paik S, Piccart M, Sridhara R, Fasching PA, Slaets L, Tang S, Gerber B, Geyer CE Jr, Pazdur R, Ditsch N, Rastogi P, Eiermann W, von Minckwitz G (2014) Pathological complete response and

long-term clinical benefit in breast cancer: the CTNeoBC pooled analysis. Lancet 384(9938):164–172. 10.1016/S0140-6736(13)62422-8 [PubMed: 24529560]

2. Gianni L, Pienkowski T, Im YHet al. (2012) Efficacy and safety of neoadjuvant pertuzumab and trastuzumab in women with locally advanced, inflammatory, or early HER2-positive breast cancer (NeoSphere): a randomised multicentre, open-label, phase 2 trial. Lancet Oncol 13:25–32 [PubMed: 22153890]
3. Hurvitz SA, Martin M, Symmans WF, Jung KH, Huang CS, Thompson AM, Harbeck N, Valero V, Stroyakovskiy D, Wildiers H, Campone M, Boileau JF, Beckmann MW, Afenjar K, Fresco R, Helms HJ, Xu J, Lin YG, Sparano J, Slamon D (2018) Neoadjuvant trastuzumab, pertuzumab, and chemotherapy versus trastuzumab emtansine plus pertuzumab in patients with HER2-positive breast cancer (KRISTINE): a randomised, open-label, multicentre, phase 3 trial. Lancet Oncol 19(1):115–126. 10.1016/S1470-2045(17)30716-7 [PubMed: 29175149]
4. Schneeweiss A, Chia S, Hickish Tet al. (2013) Pertuzumab plus trastuzumab in combination with standard neoadjuvant anthracycline-containing and anthracycline-free chemotherapy regimens in patients with HER2-positive early breast cancer: a randomized phase II cardiac safety study (TRYPHAENA). Ann Oncol 24:2278–2284 [PubMed: 23704196]
5. Krystel-Whittemore M, Xu J, Brogi E, Ventura K, Patil S, Ross DS, Dang C, Robson M, Norton L, Morrow M, Wen HY (2019) Pathologic complete response rate according to HER2 detection methods in HER2-positive breast cancer treated with neoadjuvant systemic therapy. Breast Cancer Res Treat. 10.1007/s10549-019-05295-9
6. von Minckwitz G, Huang CS, Mano MS, Loibl S, Mamounas EP, Untch M, Wolmark N, Rastogi P, Schneeweiss A, Redondo A, Fischer HH, Jacot W, Conlin AK, Arce-Salinas C, Wapnir IL, Jackisch C, DiGiovanna MP, Fasching PA, Crown JP, Wülfing P, Shao Z, Rota Caremoli E, Wu H, Lam LH, Tesarowski D, Smitt M, Douthwaite H, Singel SM, Geyer CE Jr, KATHERINE Investigators (2019) Trastuzumab Emtansine for Residual Invasive HER2-Positive Breast Cancer. N Engl J Med 380(7):617–628. 10.1056/NEJMoa1814017 [PubMed: 30516102]
7. Lehmann BD, Jovanović B, Chen X, Estrada MV, Johnson KN, Shyr Y, Moses HL, Sanders ME, Pietenpol JA (2016) Refinement of triple-negative breast cancer molecular subtypes: implications for neoadjuvant chemotherapy selection. PLoS ONE 11(6):e0157368. 10.1371/journal.pone.0157368 [PubMed: 27310713]
8. Keune JD, Jeffe DB, Schootman M, Hoffman A, Gillanders WE, Aft RL (2010) Accuracy of ultrasonography and mammography in predicting pathologic response after neoadjuvant chemotherapy for breast cancer. Am J Surg 199(4):477–484. 10.1016/j.amjsurg.2009.03.012 [PubMed: 20359567]
9. Marinovich ML, Houssami N, Macaskill P, von Minckwitz G, Blohmer JU, Irwig L (2015) Accuracy of ultrasound for predicting pathologic response during neoadjuvant therapy for breast cancer. Int J Cancer 136(11):2730–2737. 10.1002/ijc.29323 [PubMed: 25387885]
10. Candelaria RP, Bassett RL, Symmans WF, Ramineni M, Moulder SL, Kuerer HM, Thompson AM, Yang WT (2017) Performance of mid-treatment breast ultrasound and axillary ultrasound in predicting response to neoadjuvant chemotherapy by breast cancer subtype. Oncologist 22:394–401 [PubMed: 28314842]
11. von Minckwitz G, Kümmel S, Vogel P, Hanusch C, Eidtmann H, Hilfrich J, Gerber B, Huober J, Costa SD, Jackisch C, Loibl S, Mehta K, Kaufmann M, German Breast Group (2008) Intensified neoadjuvant chemotherapy in early-responding breast cancer: phase III randomized GeparTrio study. J Natl Cancer Inst. 100:552–562 [PubMed: 18398094]
12. Baumgartner A, Tausch C, Hosch S, Papassotiropoulos B, Varga Z, Rageth C, Baege A (2018) Ultrasound-based prediction of pathologic response to neoadjuvant chemotherapy in breast cancer patients. Breast 39:19–23. 10.1016/j.breast.2018.02.028 [PubMed: 29518677]
13. Hayashi N, Tsunoda H, Namura M, Ochi T, Suzuki K, Yamauchi H, Nakamura S (2019) Magnetic resonance imaging combined with second-look ultrasonography in predicting pathologic complete response after neoadjuvant chemotherapy in primary breast cancer patients. Clin Breast Cancer 19(1):71–77. 10.1016/j.clbc.2018.08.004 [PubMed: 30206035]
14. Paydary K, Seraj SM, Zadeh MZ, Emamzadehfard S, Shamchi SP, Gholami S, Werner TJ, Alavi A (2019) The evolving role of FDG-PET/CT in the diagnosis, staging, and treatment of breast cancer. Mol Imaging Biol 21(1):1–10. 10.1007/s11307-018-1181-3

15. Sheikhbahaei S, Trahan TJ, Xiao J, Taghipour M, Mena E, Connolly RM (2016) Subramaniam RM FDG-PET/CT and MRI for evaluation of pathologic response to neoadjuvant chemotherapy in patients with breast cancer: a meta-analysis of diagnostic accuracy studies. Oncologist 21(8):931–939. 10.1634/theoncologist.2015-0353 [PubMed: 27401897]
16. Tromberg BJ, Zhang Z, Leproux A, O'Sullivan TD, Cerussi AE, Carpenter PM, Mehta RS, Roblyer D, Yang W, Paulsen KD, Pogue BW, Jiang S, Kaufman PA, Yodh AG, Chung SH, Schnall M, Snyder BS, Hylton N, Boas DA, Carp SA, Isakoff SJ, Mankoff D, ACRIN 6691 investigators (2016) Predicting responses to neoadjuvant chemotherapy in breast cancer: ACRIN 6691 trial of diffuse optical spectroscopic imaging. Cancer Res 76(20):5933–5944 [PubMed: 27527559]
17. Gunther JE, Lim EA, Kim HK, Flexman M, Altoé M, Campbell JA, Hibshoosh H, Crew KD, Kalinsky K, Hershman DL, Hielscher AH (2018) Dynamic diffuse optical tomography for monitoring neoadjuvant chemotherapy in patient. Radiology 287:778 [PubMed: 29431574]
18. Tank A, Peterson HM, Pera V, Tabassum S, Leproux A, O'Sullivan T, Jones E, Cabral H, Ko N, Mehta RS, Tromberg BJ, Roblyer D (2020) Diffuse optical spectroscopic imaging reveals distinct early breast tumor hemodynamic responses to metronomic and maximum tolerated dose regimens. Breast Cancer Res 22(1):29. 10.1186/s13058-020-01262-1 [PubMed: 32169100]
19. Zhu Q, Tannenbaum S, Kurtzman SH, DeFusco P, Ricci A Jr, Vavadi H, Zhou F, Xu C, Merkulov A, Hegde P, Kane M, Wang L, Sabbath K (2018) Identifying an early treatment window for predicting breast cancer response to neoadjuvant chemotherapy using immunohistopathology and hemoglobin parameters. Breast Cancer Res 20(1):56. 10.1186/s13058-018-0975-1 [PubMed: 29898762]
20. Cochran JMet al. (2018) Tissue oxygen saturation predicts response to breast cancer neoadjuvant chemotherapy within 10 days of treatment. J Biomed Opt 24:1
21. Zhu Q, Wang L, Tannenbaum S, Ricci A Jr, DeFusco P, Hegde P (2014) Pathologic response prediction to neoadjuvant chemotherapy utilizing pretreatment near-infrared imaging parameters and tumor pathologic criteria. Breast Cancer Res 16(5):456. 10.1186/s13058-014-0456-0 [PubMed: 25349073]
22. Zhu Q, DeFusco PA, Ricci A Jr, Cronin EB, Hegde PU, Kane M, Tavakoli B, Xu Y, Hart J, Tannenbaum SH (2013) Breast cancer: assessing response to neoadjuvant chemotherapy by using US-guided near-infrared tomography. Radiology 266(2):433–442. 10.1148/radiol.12112415 [PubMed: 23264349]
23. Zhi W, Liu G, Chang C, Miao A, Zhu X, Xie L, Zhou J (2018) Predicting treatment response of breast cancer to neoadjuvant chemotherapy using ultrasound-guided diffuse optical tomography. Transl Oncol 11(1):56–64. 10.1016/j.tranon.2017.10.011 [PubMed: 29175630]
24. Jiang S, Pogue BW, Kaufman PA, Gui J, Jermyn M, Frazee TE, Poplack S, DiFlorio-Alexander R, Wells WA, Paulsen KD (2014) Predicting breast tumor response to neoadjuvant chemotherapy with diffuse optical spectroscopic tomography prior to treatment. Clin Cancer Res 20(23):6006–6015 [PubMed: 25294916]
25. Jiang S, Pogue BW (2016) A comparison of near-infrared diffuse optical imaging and 18F-FDG PET/CT for the early prediction of breast cancer response to neoadjuvant chemotherapy. J Nucl Med 57:1166 [PubMed: 27103023]
26. Tran WT, Gangeh MJ, Sannachi L, Chin L, Watkins E, Bruni SG, Rastegar RF, Curpen B, Trudeau M, Gandhi S, Yaffe M, Slodkowska E, Childs C, Sadeghi-Naini A, Czarnota GJ (2017) Predicting breast cancer response to neoadjuvant chemotherapy using pretreatment diffuse optical spectroscopic texture analysis. Br J Cancer 116(10):1329–1339. 10.1038/bjc.2017.97 [PubMed: 28419079]
27. Vavadi H, Mostafa A, Zhou F, Uddin KMS, Althobaiti M, Xu C, Bansal R, Ademuyiwa F, Poplack S, Zhu Q (2018) Compact ultrasound-guided diffuse optical tomography system for breast cancer imaging. J Biomed Opt 24(2):1–9. 10.1117/1.JBO.24.2.021203
28. Uddin KMS, Mostafa A, Anastasio M, Zhu Q (2017) Two step imaging reconstruction using truncated pseudoinverse as a preliminary estimate in ultrasound guided diffuse optical tomography. Biomed Opt Express 8(12):5437–5449. 10.1364/BOE.8.005437 [PubMed: 29296479]
29. Ogston KN, Miller ID, Payne Set al. (2003) A new histologic grading system to assess response of breast cancers to primary chemotherapy; prognostic significance and survival. Breast 12:320–327 [PubMed: 14659147]

30. Symmans WF, Peintinger F, Hatzis Cet al. (2007) Measurement of residual breast cancer burden to predict survival after neoadjuvant chemotherapy. J Clin Oncol 25:4414–4422 [PubMed: 17785706]
31. Harvey JM, Clark GM, Osborne CK, Allred DC (1999) Estrogen receptor status by immunohistochemistry is superior to the ligand-binding assay for predicting response to adjuvant endocrine therapy in breast cancer. J Clin Oncol 17(5):1474–1481 [PubMed: 10334533]
32. Nonparametric Statistics: a step-by-step approach, Gregory WCorder and Dole I. Foreman (2009).
33. Heller G, Seshan VE, Moskowitz CS, Gonen M (2016) Inference for the difference in the area under the ROC curve derived from nested binary regression models. Biostatistics 18:260–274
34. Kruppa J, Liu Y, Biau G, Kohler M, König IR, Malley JD, Ziegler A (2014) Probability estimation with machine learning methods for dichotomous and multicategory outcome: theory. Biom J 56(4):534–563. 10.1002/bimj.201300068 [PubMed: 24478134]
35. Dobruch-Sobczak K, Piotrzkowska-Wróblewska H, Klimonda Z, Roszkowska-Purska K (2019) Litniewski ultrasound echogenicity reveals the response of breast cancer to chemotherapy. J Clin Imaging 55:41–46. 10.1016/j.clinimag.2019.01.021
36. Matsuda N, Kida K, Ohde S, Suzuki K, Yamauchi H, Nakamura S, Tsunoda H (2018) Change in sonographic brightness can predict pathological response of triple-negative breast cancer to neoadjuvant chemotherapy. Breast Cancer 25(1):43–49. 10.1007/s12282-017-0782-z [PubMed: 28536943]
37. Zhao Y, Dong X, Li R, Ma X, Song J, Li Y, Zhan D (2015) Evaluation of the pathological response and prognosis following neoadjuvant chemotherapy in molecular subtypes of breast cancer. Onco Targets Ther 8:1511–1521 [PubMed: 26150728]
38. Sejben A, Kószó R, Kahán Z, Cserni G, Zombori T (2020) Examination of tumor regression grading systems in breast cancer patients who received neoadjuvant therapy. Pathol Oncol Res 26(4):2747–2754. 10.1007/s12253-020-00867-3 [PubMed: 32691390]
39. Masuda N, Lee SJ, Ohtani S, Im YH, Lee ES, Yokota I, Kuroi K, Im SA, Park BW, Kim SB, Yanagita Y, Ohno S, Takao S, Aogi K, Iwata H, Jeong J, Kim A, Park KH, Sasano H, Ohashi Y, Toi M (2017) Adjuvant capecitabine for breast cancer after preoperative chemotherapy. N Engl J Med 376(22):2147–2159. 10.1056/NEJMoa1612645 [PubMed: 28564564]

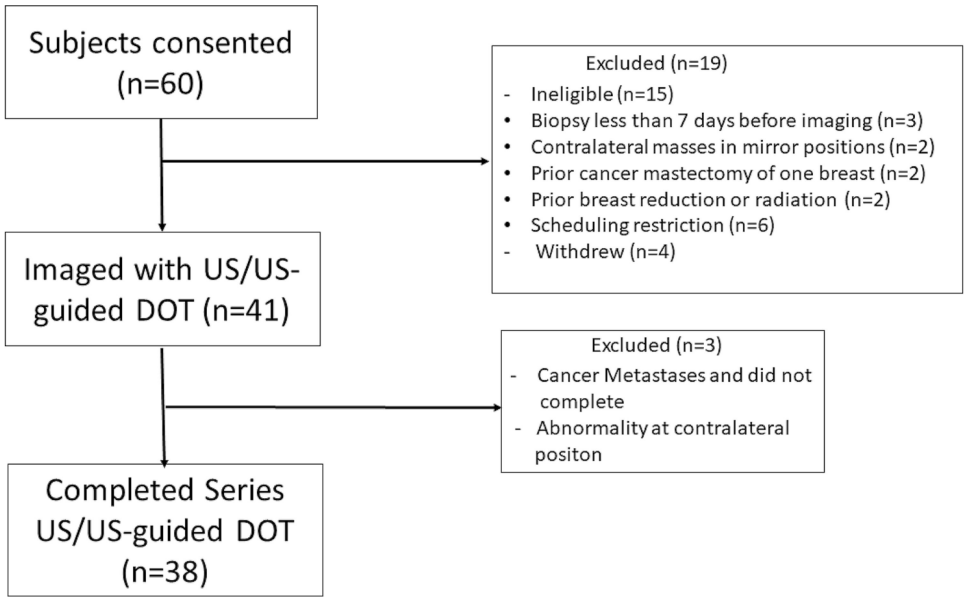

Fig. 1.

Patient Study Flow Diagram. Exclusion criteria included pregnancy, breastfeeding, prior history of breast cancer, prior history of chest wall radiation, prior history of breast reconstruction, reduction, or augmentation and bilateral breast cancers

Fig. 2.

US-guided DOT probe. The foot-print of the combined DOT probe is approximately 10 cm. Four source laser diodes of 730 nm, 785 nm, 808 nm and 830 nm optical wavelengths were sequentially switched to nine source positions (pointed by an arrow) on the probe, while the reflected light was coupled by the 14 light guides (pointed by an arrow) to 14 parallel detectors

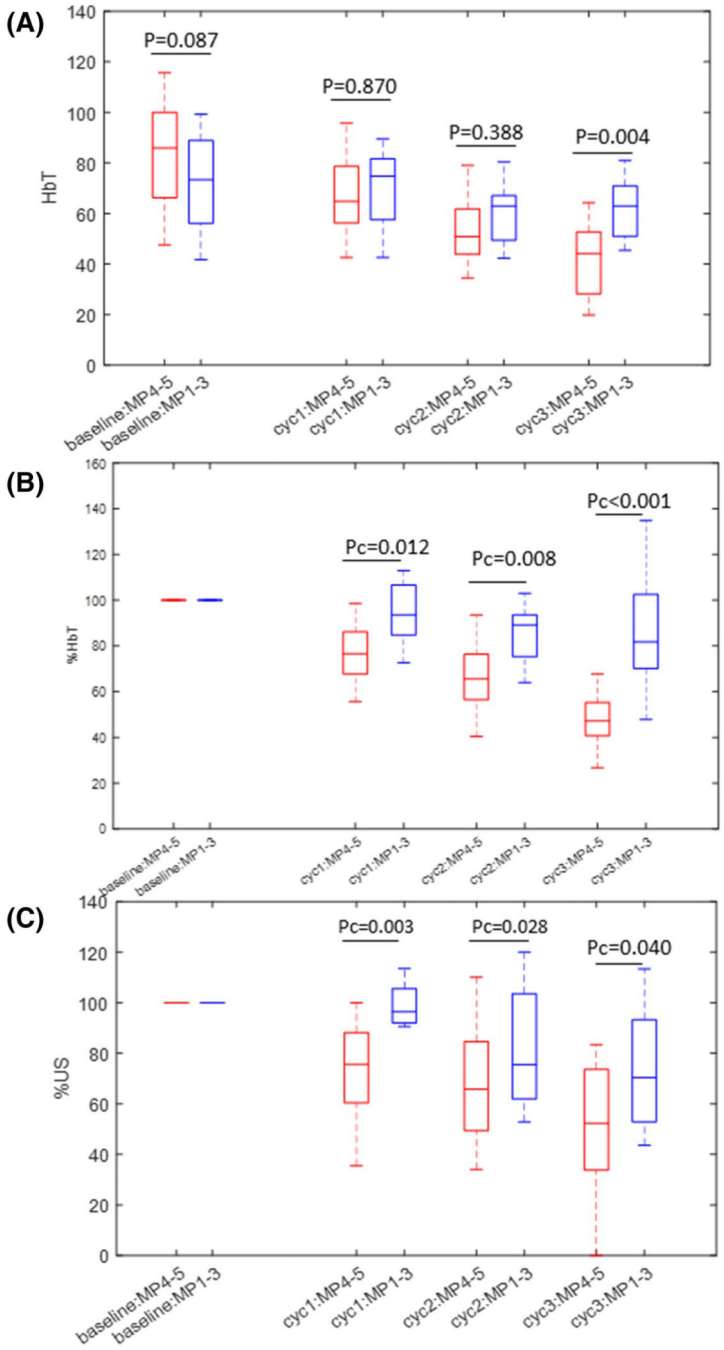

Fig. 3.

a HbT of Miller-Payne grade 4–5 tumors (therapy responders) and grade 1–3 tumors after 1, 2, 3 cycles of neoadjuvant therapy. The unit is μM. **b** %HbT of grade 4–5 tumors vs. grade 1–3 tumors after first three cycles of neoadjuvant therapy. **c** %US of grade 4–5 tumors vs. grade 1–3 tumors after first three cycles of neoadjuvant therapy. *P*c is Bonferroni-Holm corrected *P* value

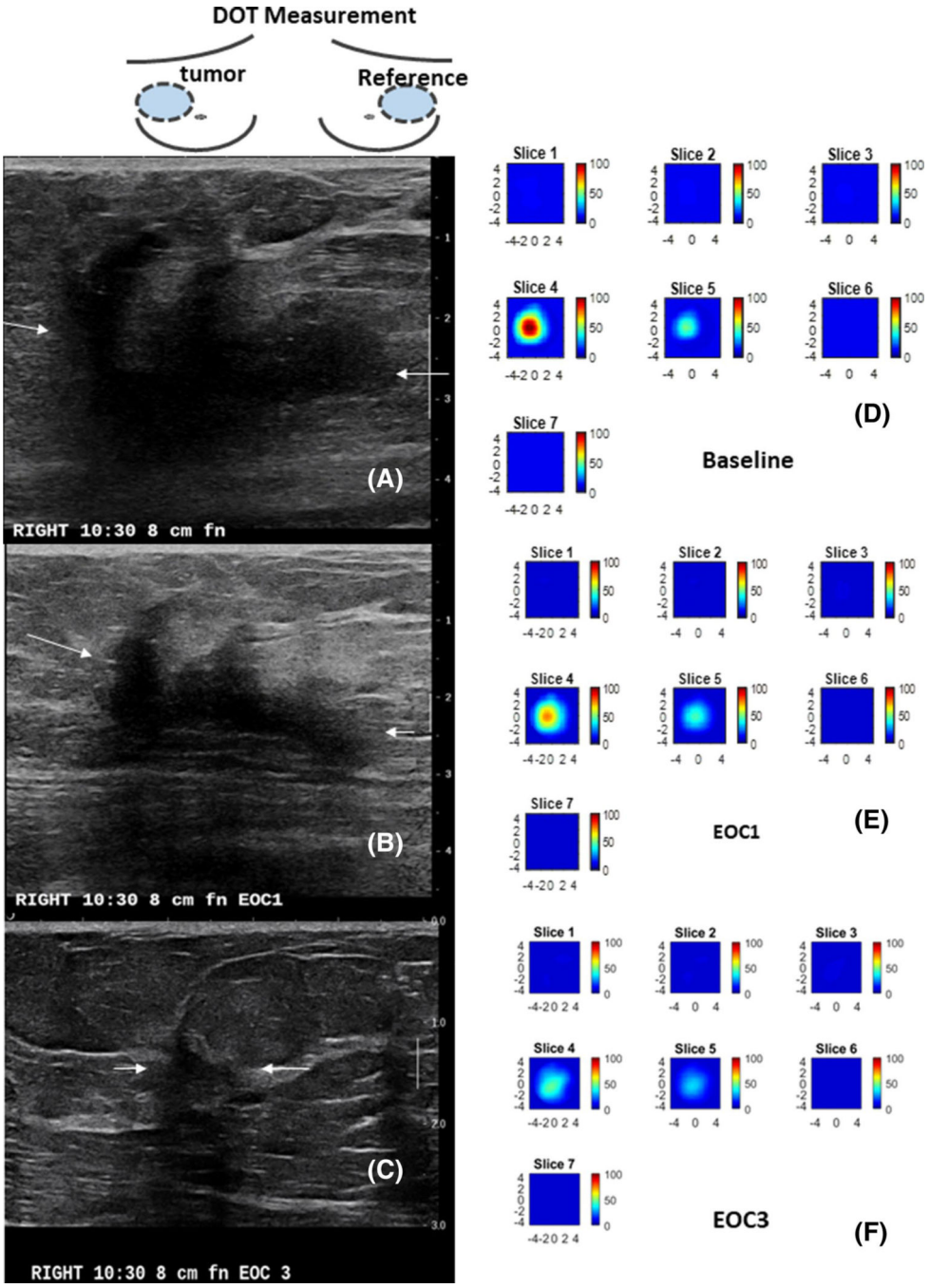

Fig. 4.

A 59 year-old patient with a T3 triple negative cancer and treated with ACT. The US/DOT imaging were performed at baseline, end of cycle 1 (EOC1), 2, 3, 5 and before surgery. **a**–**c** are co-registered US images obtained at baseline, EOC1 and EOC3. The largest lesion diameters measured by US were 4.6 cm, 3.4 cm, 1.0 cm. The corresponding %US at EOC1 and EOC 3 were 73.9% and 21.7%. **e**–**f** are corresponding HbT maps. Each map has 7 slices reconstructed at depths from 0.5 cm to 3.5 cm with 0.5 cm spacing. Each slice has spatial dimensions of 9 cm by 9 cm. The maximum HbT measured at baseline, EOC1, and EOC3

were 108.7 μM, 73.5 μM, and 45.0 μM. The %HbT were 67.6% and 41.4% at EOC1 and EOC3. The patient achieved pCR with Miller-Payne of 5

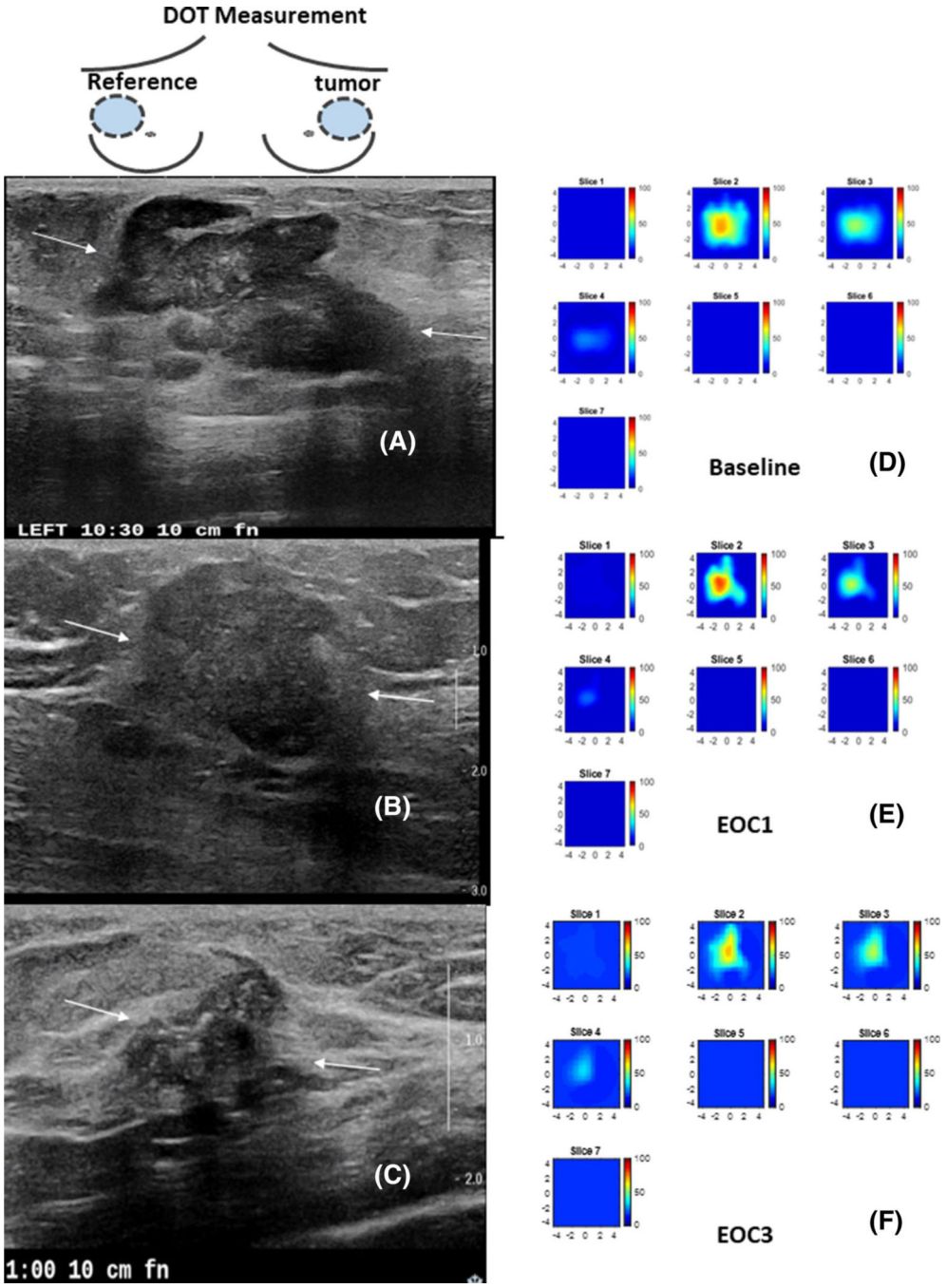

Fig. 5.

A 62 year-old patient with a T2 ER negative PR positive and HER2 negative IDC and treated with ACT. The US/DOT imaging were performed at baseline, end of cycle 1, 2, 3 and before surgery. **a**–**c** are co-registered US images obtained at baseline, EOC1 and EOC3. The largest lesion diameters measured by US were 3.6 cm, 2.4 cm, 1.7 cm. The corresponding %US at EOC1 and EOC 3 were 66.7% and 47.2%. **e**–**f** are corresponding HbT maps. Each map has 7 slices reconstructed at depths from 0.5 cm to 3.5 cm with 0.5 cm spacing. Each slice has a spatial dimensions of 9 cm by 9 cm. The maximum HbT measured at baseline, EOC1, and

EOC3 were 70.3 μM, 79.3 μM, and 65.8 μm. The %HbT were 112.8% and 93.6% at EOC1 and EOC3. The patient had 2.4 cm residual tumor with no histologic evidence of tumor response as evaluated after the surgery. Miller-Payne grade was 1

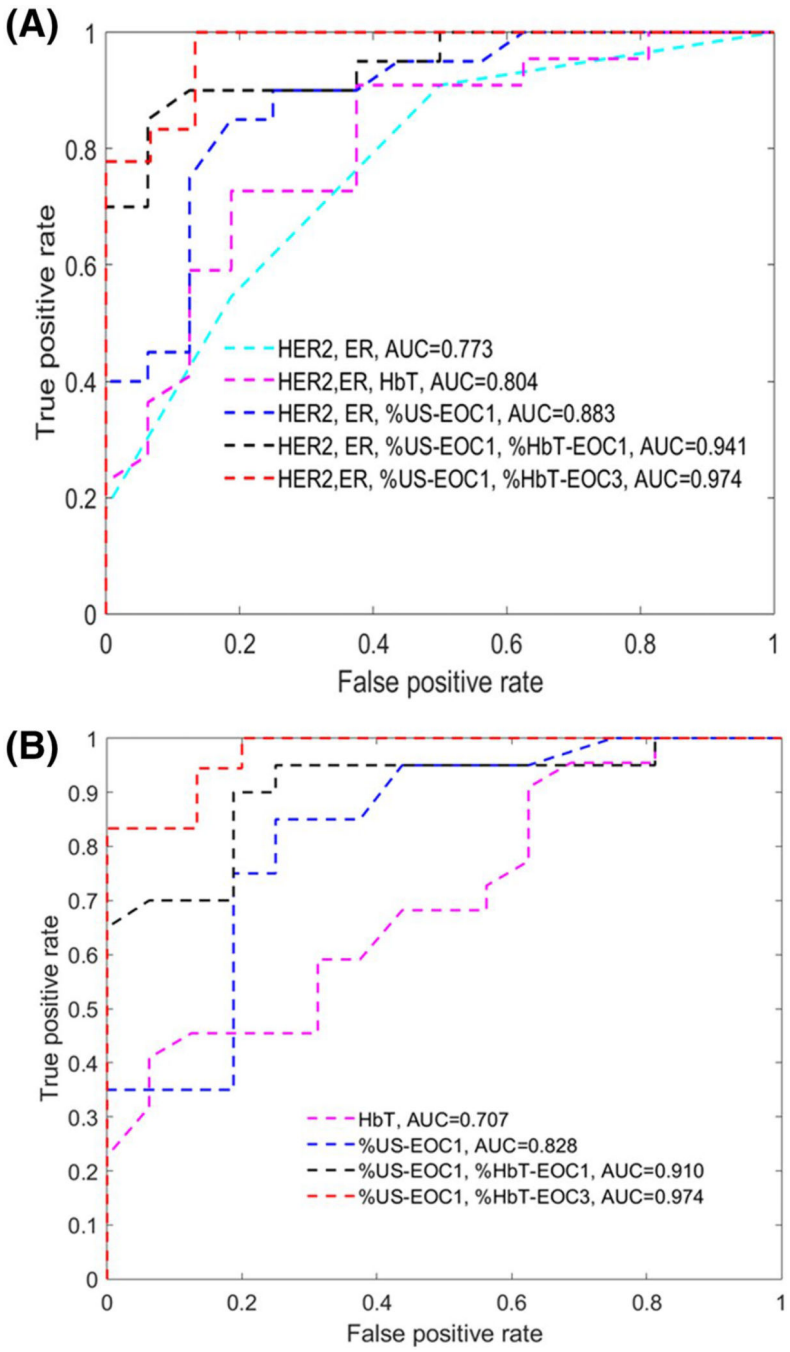

Fig. 6.

ROCs obtained from different set of predictor variables. **a** ROCs of known HER2/ER subgroup with 5 sets of predictor variables, and **b** ROCs based on HbT, %US-EOC1, %HbT and %US changes regardless of biomarkers

Table 1

Clinicopathologic characteristics, biomarkers, initial (clinical) tumor staging and primary baseline tumor size measured by US, (post-neoadjuvant) residual gross tumor size, residual cancer burden, post-treatment tumor size measured by US, treatment regimens, and Miller-Payne (MP) grade

Subject #	Age	Histology type	Grade[1] score	Biological subtype	Tumor stage/ US tumors (cm)	Residual tumor (cm) (gross)/RCB index	US Tumor size (post) (cm)	Treatment regimen	MP grade
NIR005	40	IDC	Intermed (6)	ER + PR + HER2−	T2/2.6	2.1/2.796	1.2	ACT	3
NIR006	44	IDC	High (9)	ER-PR-HER2−	T2/2.2	0.0/0.0	0.3	ACT	5
NIR008	31	IDC	High (9)	ER + PR + HER2−	T2/2.1	0.8/2.73	0.8	ACT	3
NIR011	45	IDC	High (9)	ER-PR-HER−	T2/2.1	0.0/0.0	1.1	ACT	5
NIR014	38	IDC	Intermed (6)	ER + PR + HER2−	T2/5.2	2.5/3.19	0.5	ACT	2
NIR015	61	IDC	High (9)	ER-PR + HER2−	T2/3.6	2.4/2.368	1.0	ACT	1
NIR021	59	IDC	High (8)	ER-PR-HER−	T1/1.0	0.0/0.0	0.4	ACT	5
NIR023	65	IDC	High (9)	ER-PR-HER2−	T2/1.9	0.3/1.333	0.7	ACT	3
NIR025	59	IDC	High (9)	ER-PR-HER2−	T3/4.6	0.0/0.0	0.4	ACT	5
NIR026	45	IDC	High (9)	ER + PR + HER2−	T2/3.1	0.7/1.355	3.4	ACT	4
NIR027	41	IDC	High (9)	ER + PR-HER−	T2/3.9	3.1/3.52	2.1	ACT	1
NIR034	35	IDC	High (8)	ER + PR + HER2−	T2/3.1	1.2/2.953	1.0	ACT	2
NIR038	44	IDC	Intermed (5)	ER + PR + HER2−	T3/2.0	2.0/4.024	1.9	ACT	3
NIR041	48	ILC	Intermed (5)	ER + PR + HER−	T3/4.5	4.1/4.251	3.9	ACT	1
NIR001	62	IDC	High (8)	ER + PR + HER2 +	T2/1.2	0.0/0.0	0.0	TCHP	5
NIR003	48	IMC	Intermed (4)	ER + PR + HER2 +	T2/2.9	2.9/1.642	3.0	TCHP	1
NIR007	42	IDC	High (9)	ER- PR-HER2 +	T3/3.0	0.0/0.0	2.5	TCHP	5
NIR010	39	IDC	High (9)	ER + PR-HER2 +	T2/3.0	0.0/0.0	0.5	TCHP	5
NIR018	44	IDC	High (7)	ER-PR- HER2 +	T2/4.3	0.0/0.0	1.8	TCHP	5
NIR019	37	IDC	High (9)	ER + PR + Her2 +	T2/4.7	0.0/0.0	1.9	TCHP	5
NIR022	30	IDC	High (9)	ER-PR-HER2 +	T2/2.7	0.0/0.0	0.0	TCHP	5
NIR029	52	IDC	High (8)	ER + PR-HER2 +	T2/2.2	0.0/0.0	1.4	TCHP	5
NIR032	38	IDC	Intermed (6)	ER + PR-HER2 +	T3/1.9	0.0/0.0	1.2	TCHP	5
NIR035	50	IDC	High (7)	ER-PR-HER2 +	T1/2.5	0.0/0.0	0.0	TCHP	5
NIR040	34	IDC	High (7)	ER + PR + HER +	T2/4.8	0.2/1.277	0.8	TCHP	4
NIR004	50	IDC	High (9)	ER-PR-HER2−	T3/2.0	0.0/0.0	1.6	CarboT	5

Subject #	Age	Histology type	Grade[1] score	Biological subtype	Tumor stage/ US tumors (cm)	Residual tumor (cm) (gross)/RCB index	US Tumor size (post) (cm)	Treatment regimen	MP grade
NIR009	38	IDC	High (8)	ER-PR + HER-PR + HER2−	T2/1.4	0.0/0.0	0.0	CarboT	5
NIR016	53	IDC	High (9)	ER + [2]PR-HER2−	T2/2.3	0.0/0.0	1.1	CarboT	5
NIR020	48	IDC	High (7)	ER-PR-HER2−	T2/2.7	0.15/1.899	1.9	CarboT	3
NIR030	71	IDC	High (9)	ER-PR-HER2−	T2/3.8	0.9/2.045	1.8	CarboT	2
NIR031	24	IDC	High (9)	ER-PR-HER2−	T3/3.4	0.0/0.0	0.5	CarboT-AC	5
NIR012	49	IDC	High (9)	ER- PR-HER2−	T2/2.2	0.0/0.0	2.3	ACP	5
NIR028	39	IDC	High (8)	ER-PR-HER2−	T2/2.8	2.5/3.82	2.4	ACP	3
NIR013	52	IDC	High (9)	ER + PR-HER2 +	T3/6.8	1.3/1.59	n/a[3]	PLT	3
NIR033	56	IDC/ILC	High (9)	ER + PR-HER2 +	T2/4.1	1.1/1.561	2.4	PLT	3
NIR036	57	IDC	High (8)	ER + PR + HER2 +	T2/2.2	0.1/0.598	1.4	PLT	4
NIR037	43	IDC	High (7)	ER + PR + HER2 +	T1/2.3	0.0/0.0	1.3	PLT	5
NIR039	66	IDC	Intermed (5)	ER + PR + HER2−	T2/3.1	1.5/3.222	n/a[3]	Anastrazole	1

IDC invasive ductal carcinoma, *IMC* invasive mucinous carcinoma, *ILC* invasive lobular carcinoma, *TCHP* docetaxel, carboplatin, trastuzumab, and pertuzumab, *ACT* AC (Doxorubicin hydrochloride and cyclophosphamide) every two weeks followed by weekly paclitaxel (Taxol) for 12 weeks, *CarboT* carboplatin (paraplatin) and docetaxel (taxotere), ClinicalTrials.gov Identifier: NCT02124902, *ACP* atezolizumab carboplatin paclitaxel ClinicalTrials.gov Identifier: NCT02883062, *PLT* Palbociclib Letrozole Trastuzumab ClinicalTrials.gov Identifier: NCT02907918, *CarboT-AC* carboplatin and docetaxel for four cycles followed by doxorubicin (adriamycin) / cyclophosphamide

[1] Nottingham Grade: 1–3 low, 4–6 intermediate, 7–9 high

[2] Initial receptor report from outside hospital was TNBC and corrected later as ER +

[3] Surgery earlier than scheduled

Table 2

Spearman's rho correlation coefficient and *P* value between Miller-Payne grade and tumor Nottingham grade, tumor subtypes (HER2, ER, TNBC), pre-treatment HbT, oxyHb, deoxyHb, %HbT measured at end of cycles (EOCs) 1–3 and post-treatment HbT and %HbT. Pre-treatment US, %US measured at the end of cycle 1–3, and post-treatment US and %US

Predictors		
Biomarkers	**US predictors**	**Hemoglobin predictors**
Nottingham grade rho = 0.260 (*P* = 0.115) HER2 rho = 0.336 (*P* = 0.039) ER rho = 0.341 (*P* = 0.036) TNBC rho = 0.245 (*P* = 0.138)	Pre-treatment US rho = − 0.408 (*P* = 0.011) %US_EOC1 rho = − 0.461 (*P* = 0.005) %US_EOC2 rho = − 0.346 (*P* = 0.045) %US_EOC3 rho = − 0.420 (*P* = 0.013) Post-treatment US rho = − 0.416 (*P* = 0.012) Post-treatment %US rho = − 0.270 (*P* = 0.111)	Pre-treatment HbT rho = 0.358 (*P* = 0.028) Pre-treatment oxyHb rho = 0.278 (*P* = 0.091) Pre-treatment deoxyHb rho = 0.249 (*P* = 0.132) %HbT_EOC1 rho = − 0.513 (*P* = 0.001) %HbT_EOC2 rho = − 0.587 (*P* < 0.001) %HbT_EOC3 rho = − 0.731 (*P* < 0.001) Post-treatment HbT rho = − 0.094 (*P* = 0.592) Post-treatment %HbT rho = − 0.445 (*P* = 0.007)

Data were from this study of total 38 patients

Table 3

Spearman's rho correlation coefficients of the treatment prediction variables

	ER	HbT	%Hb_EOC1	%HbT_EOC2	%HbT_EOC3	US	%US_EOC1	%US_EOC2	%US_EOC3
HER2	−0.293	0.263	− 0.052	− 0.114	− 0.386	0.118	− 0.404	− 0.241	− 0.130
ER		0.171	− 0.129	− 0.210	− 0.196	− 0.191	− 0.164	− 0.222	− 0.269
TN		0.000	− 0.154	− 0.194	− 0.131	− 0.305	0.099	0.016	− 0.135
HbT			− 0.449	− 0.582	− 0.463	− 0.015	− 0.167	− 0.180	0.234
%HbT_EOC1				**0.701** *	**0.641**	0.151	− 0.076	0.037	0.104
%HbT_EOC2					**0.644**	− 0.039	0.192	0.142	0.239
%HbT_EOC3						0.202	0.282	0.220	0.399
US							− 0.111	− 0.178	− 0.060
%US_EOC1								**0.792**	**0.641**
%US_EOC2									**0.875**
%US EOC3									

Data were from this study of total 38 patients

*The high correlation coefficients occur between %HbT_EOC1, %HbT_EOC2 and %HbT_EOC3, and between %US_EOC1, %US_EOC2, and %US_EOC3

Table 4

Logistic regression analysis based on tumor subtypes (HER2, ER) and TNBC, US measurements, and hemoglobin parameters, AUC ROC Analysis including HER2 and ER Biomarker status

ROC Analysis including HER2 and ER Biomarker status			
Biomarkers, HbT measured before NAT	Biomarkers, %US measured at EOCs 1–3	Biomarkers, HbT, %HbT measured at EOCs 1–3	Biomarkers, %HbT and %US measured at EOCs 1–3
HER2, ER AUC = 0.773 95% CI: 0.629–0.917 HER2, ER, HbT AUC = 0.804 95% CI: 0.659–0.949 TNBC AUC = 0.557 95% CI: 0.407–0.707	HER2, ER, %US_EOC1 AUC = 0.883 95% CI: 0.768–0.997 HER2, ER, %US_EOC2 AUC = 0.771 95% CI: 0.608–0.935 HER2, ER, %US_EOC3 AUC = 0.842 95% CI: 0.710–0.975	HER2, ER, HbT, %HbT_EOC1 AUC = 0.903 95% CI: 0.808–0.998 HER2, ER, HbT, %HbT_EOC2 AUC = 0.911 95% CI: 0.811–1.0 HER2, ER, HbT, %HbT_EOC3 AUC = 0.968 95% CI:0.918–1.0	**HER2,ER,%HbT_EOC1,%US_EOC1** **AUC = 0.941** **95% CI: 0.869–1.0** HER2, ER, %HbT_EOC2, %US_EOC2 AUC = 0.900 95% CI: 0.797–1.0 HER2, ER, %HbT_EOC3, %US_EOC3 AUC = 0.968 95% CI: 0.918–1.0 **HER2, ER, %HbT_EOC3,%US_EOC1** **AUC = 0.974*** **95% CI: 0.932–1.0**
ROC Analysis using imaging parameters only			
US and HbT measured before NAT	%US measured at EOCs 1–3	%HbT measured EOCs 1–3	%HbT and %US measured at EOCs 1–3
US AUC = 0.671 95% CI: 0.492–0.849 HbT AUC = 0.707 95% CI:0.540–0.8744	%US_EOC1 AUC = 0.828 95% CI: 0.685–0.971 %US_EOC2 AUC = 0.679 95% CI: 0.489–0.869 %US_EOC3 AUC = 0.723 95% CI: 0.547–0.898	HbT, %HbT_EOC1 AUC = 0.825 95% CI: 0.684–0.966 HbT, %HbT_EOC2 AUC = 0.839 95% CI: 0.706–0.973 HbT, %HbT_EOC3 AUC = 0.944 95% CI: 0.870–1.0	**%HbT_EOC1, %US_EOC1** **AUC = 0.910*** 95% CI: 0.810–1.0 %HbT_EOC2, %US_EOC2 AUC = 0.889 95% CI: 0.774–0.993 %HbT_EOC3,%US_EOC3 AUC = 0.944 95% CI: 0.870–1.0 **%HbT_EOC3%, US_EOC1** **AUC = 0.974*** **95% CI: 0.933–1.0**

Data were from this study of total 38 patients

*Best prediction at early treatment points

Table 5

Generalized logistic regression parameters β_n, n = 0, 1,2, 3,.. of selected models given in Fig. 6

	HER2	ER	HbT	%US_EOC1	%HbT_EOC1	%HbT_EOC3
HER2, ER	2.561	2.026				
HER2, ER, HbT	2.342	1.866	0.027			
HER2, ER, %US-EOC1	2.442	2.102		− 0.056		
HER2, ER, %US_EOC1, %HbT_EOC1	2.010	2.179		− 0.0711	− 0.075	
HER2, ER, %US_EOC1, %HbT_EOC3	− 0.121	3.079		− 0.098	− 0.196	
HbT			0.038			
%US_EOC1				− 0.078		
%US_EOC1, %HbT_EOC1				− 0.093		− 0.077
%US_EOC1, %HbT_EOC3				− 0.078		− 0.134

Data were from this study of total 38 patients